New Structural Model for Mixed-Chain Phosphatidylcholine Bilayers†

T. J. McIntosh,* S. A. Simon, J. C. Ellington, Jr., and N. A. Porter

ABSTRACT: Multilamellar suspensions of a mixed-chain saturated phosphatidylcholine with 18 carbon atoms in the *sn*-1 chain and 10 carbon atoms in the *sn*-2 chain have been analyzed by X-ray diffraction techniques. The structural parameters for this lipid in the gel state are quite different than usual phosphatidylcholine bilayer phases. A symmetric and sharp wide-angle reflection at 4.11 Å indicates that the hydrocarbon chains in hydrated C(18):C(10)PC bilayers are more tightly packed than in usual gel-state phosphatidylcholine bilayers and that there is no hydrocarbon chain tilt. The lipid thickness is about 12 Å smaller than would be expected in a normal bilayer phase, and the area per molecule is 3 times the area per hydrocarbon chain. In addition, the bilayer thickness increases upon melting to the liquid-crystalline state, whereas normal bilayer phases decrease in thickness upon melting. On the basis of these data, we propose a new lipid packing model for gel-state C(18):C(10)PC bilayers in which the long C(18) chain spans the entire width of the hydrocarbon region of the bilayer and the short C(10) chain aligns or abuts with the C(10) chain from the apposing molecule. This model is novel in that there are three hydrocarbon chains per head group at the lipid–water interface. Calculations show that this phase is energetically favorable for mixed-chain lipids provided the long acyl chain is nearly twice the length of the shorter chain. In the liquid-crystalline state C(18):C(10)PC forms a normal fluid bilayer, with two chains per head group. The data suggest that in this melted phase significant acyl chain interdigitation across the geometric center of the bilayer is likely due to the mismatch in chain lengths.

Many biological membrane lipids are asymmetric in that one acyl chain contains more methylene groups than the other. For example, in lipids such as sulfatides, cerebrosides, and sphingomyelins, the acyl chains may differ by as many as 6–10 carbons per chain (O'Brien & Rouser, 1964; DeVries & Norton, 1974; Barenholz & Thompson, 1980; Calhoun & Shipley, 1979). In spite of this asymmetry in naturally occurring lipids, most studies involving model membranes have used symmetric lipids such as C(14):C(14)PC and C(16):C(16)PC.[1] However, mixed-chain phosphatidylcholines have recently been synthesized and analyzed by differential scanning calorimetry (Mason et al., 1981) and Raman spectroscopy (Huang et al., 1983). Huang and colleagues have found that the transition entropy (Mason et al., 1981) and change in Raman spectral indices for both the C–C and C–H stretching regions across the main order/disorder transition (Huang et al., 1983) are significantly different for mixed-chain and symmetric phosphatidylcholines. For mixed-chain phosphatidylcholines with the *sn*-1 acyl chain fixed in length at 18 carbon atoms and the *sn*-2 acyl chain length varying in steps of two methylene units from 10 to 18 carbon units, they found a maximum order/disorder change for C(18):C(10)PC and a minimum change for C(18):C(14)PC (Mason et al., 1981; Huang et al., 1983). Using these data, Mason et al. (1981) and Huang et al. (1983) have proposed a structural model for these mixed-chain dispersions with a bilayer arrangement in which the long chain of each lipid molecule crosses the geometric center of the bilayer and aligns with the short chain of the apposing lipid molecule. That is, the acyl chains are interdigitated only to the extent of the mismatch in chain lengths. This type of packing model is consistent with the X-ray diffraction data of Tardieu et al. (1973) for C(18):C(10)PC at very low (1%) water content.

In the present paper, we investigate, by X-ray diffraction, the structure of two mixed-chain lipids, C(18):C(10)PC and C(18):C(14)PC, under a range of hydration conditions. We find that hydrated gel-state C(18):C(14)PC forms bilayers with tilted hydrocarbon chains such as the $L_{\beta'}$ phase (Tardieu et al., 1973) of symmetric saturated phosphatidylcholines. However, the X-ray data indicate that C(18):C(10)PC forms a quite different type of gel-state bilayer when fully hydrated or for water contents greater than 10%. In this hydrated C(18):C(10)PC bilayer, the chains are not tilted, the bilayer is about 12 Å less than would be predicted by the Mason et al. (1981) model, and the area per molecule is 3 times the area per hydrocarbon chain, as contrasted with the value of 2 expected for a normal bilayer. Moreover, the lipid thickness increases upon melting to the liquid-crystalline state. We propose a structural model for this gel phase where the long C(18) chain extends across the entire hydrocarbon width of the bilayer and the short C(10) chain aligns with the C(10) chain of the apposing molecule in the center of the bilayer. Even though the long hydrocarbon chain is exposed to interfacial water in this conformation, our calculations show that this packing arrangement is energetically favorable because the hydrocarbon chains pack closer than in a normal bilayer. The model is consistent with all of the X-ray data, as well as with the calorimetry data of Mason et al. (1981) and Raman spectroscopy data of Huang et al. (1983).

In the liquid-crystalline phase the area per molecule for C(18):C(10)PC is somewhat smaller, and the partial lipid thickness is larger than for melted C(14):C(14)PC. We interpret these data to suggest that above the phase transition temperature the lipid pack in a fluid bilayer L_α phase (Tardieu

† From the Departments of Anatomy (T.J.M.), Physiology (S.A.S.), and Anesthesiology (S.A.S.), Duke University Medical Center, Durham, North Carolina 27710, and the Department of Chemistry (J.C.E. and N.A.P.), Duke University, Durham, North Carolina 27706. *Received January 10, 1984.* This work was supported by a grant from the National Institutes of Health (GM-27278) and by a grant from the Walker P. Inman Fund. An abstract of this work was presented at the Biophysical Society Meeting, San Antonio, TX, 1984 (McIntosh et al., 1984).

[1] Abbreviations: C(14):C(14)PC, L-α-dimyristoylphosphatidylcholine; C(16):C(16)PC, L-α-dipalmitoylphosphatidylcholine; C(18):C(18)PC, L-α-distearoylphosphatidylcholine; C(18):C(10)PC, 1-stearoyl-2-caproyl-*sn*-glycero-3-phosphocholine; C(18):C(14)PC, 1-stearoyl-2-myristoyl-*sn*-glycero-3-phosphocholine; C(10):C(18)PC, 1-caproyl-2-stearoyl-*sn*-glycero-3-phosphocholine; RP-HPLC, reversed-phase high-performance liquid chromatography.

0006-2960/84/0423-4038$01.50/0

et al., 1973) with two chains per group at the interface but with significant acyl chain penetration or interdigitation into the apposing monolayer. This interdigitation would tend to couple the two monolayers of the bilayer.

Materials and Methods

C(18):C(14)PC was used as obtained from Avanti Biochemicals. C(18):C(10)PC was synthesized according to the procedures of Mason et al. (1981). Briefly, 1 equiv of 1-stearoyllyso-PC, freshly prepared by phospholipase A_2 hydrolysis of C(18):C(18)PC, and 5 equiv of decanoic anhydride along with 1.1 equiv of 4-pyrrolidinopyridine were reacted in chloroform at 37 °C. After 2 h the acylation reaction was deemed complete by monitoring of normal-phase TLC. A 74% yield of C(18):C(10)PC was obtained after normal-phase HPLC purification on a Waters System Preparative 500 system. Proton NMR analysis showed 72 protons, 54 belonging to the acyl chains, 5 associated with the glycerol moiety, and 13 being phosphatidylcholine protons, consistent with the proposed chemical composition. A retention volume similar to another 28-carbon diacyl analogue, C(14):C(14)PC, was observed by RP-HPLC analysis. In order to determine the extent of isomerization of the acyl chains, a partial hydrolysis at the glycerol C-2 of C(18):C(10)PC was accomplished with phospholipase A_2. The free fatty acid was extracted from the reaction mixture with a 1/1 mixture of diethyl ether and hexane. The fatty acid methyl esters were formed upon addition of a 3% HCl/methanol solution. The remaining lyso-PC was transesterified by 1 N KOH/methanol, giving the fatty acid methyl ester. Gas chromatographic analysis of the methyl esters yielded the following results: >97% capric acid at glycerol carbon 2 of C(18):C(10)PC and >99% stearic acid at glycerol carbon 1 of C(18):C(10)PC.

Samples for X-ray diffraction were prepared by weighing dry lipid into small conical glass containers and adding a measured amount of doubly distilled water. The specimens were covered with argon, vortexed, and allowed to equilibrate above the lipid's main phase transition temperature for several hours. The specimens were then sealed in quartz glass X-ray capillary tubes and mounted in a temperature-regulated specimen holder in a pinhole collimation X-ray camera containing three sheets of Kodak NS-5T X-ray film in a flat plate film cassette. Specimen-to-film distances were usually 10 cm, and exposure times were of 3–7 h. The films were processed by standard techniques and densitometered with a Joyce-Loebl microdensitometer, Model MKIIIC. The background curve was subtracted, and integrated intensities $I(h)$, where h is the diffraction order, were obtained as previously described (McIntosh, 1980). For these unoriented specimens, the structure amplitude for order h was set equal to $[h^2I(h)]^{1/2}$.

Results

Typical X-ray diffraction patterns are shown in Figure 1 from partially hydrated C(18):C(10)PC and C(18):C(14)PC multilayers below their main transition and pretransition temperatures of 19.7 and 19.1 °C, respectively (Mason et al., 1981). In both cases the low-angle reflections are typical of lamellar phases. For C(18):C(14)PC the wide-angle pattern contains a sharp reflection at 4.21 Å surrounded by a broad band centered about 4.1 Å. This type of wide-angle pattern is characteristic of Lβ' phase bilayers with tilted hydrocarbon chains (Tardieu et al., 1973). The Lβ' phase is present in many symmetric, saturated phosphatidylcholines below their pretransition temperatures (Tardieu et al., 1973; Janiak et al., 1979; McIntosh, 1980). The wide-angle pattern for C(18):C(10)PC is different in that it contains a sharp, symmetric

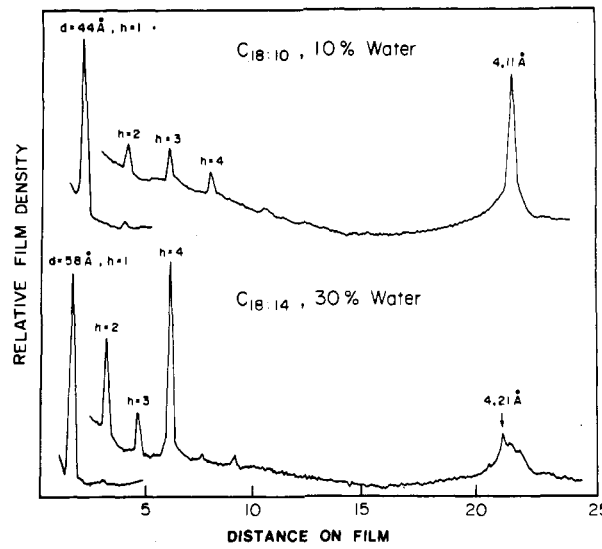

FIGURE 1: Densitometer traces of X-ray diffraction patterns from C(18):C(10)PC in 10% water at T = 13 °C and from C(18):C(14)PC in 30% water at T = 13 °C. Four lamellar orders are seen in each trace. The wide-angle pattern for C(18):C(10)PC consists of a sharp symmetric reflection at 4.11 Å, whereas for C(18):C(14)PC there is a sharp reflection at 4.21 Å and a broad band at about 4.1 Å.

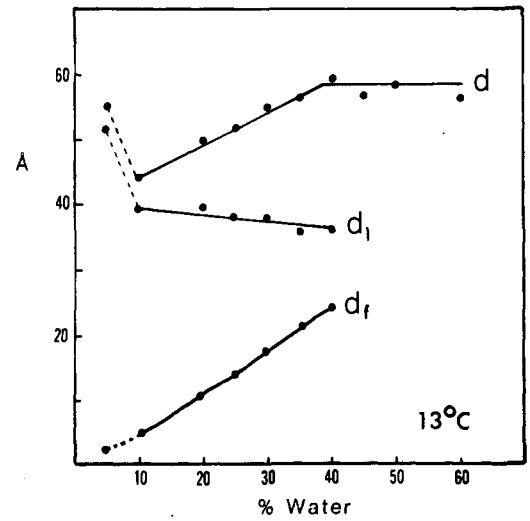

FIGURE 2: Repeat period (d), partial thickness of lipid layer (d_l), and fluid layer thickness (d_f) for C(18):C(10)PC at 13 °C.

reflection at d_s = 4.11 Å (Figure 1). An additional weak reflection is also observed at 2.37 Å, which is equal to $d_s/3^{1/2}$. This type of pattern is characteristic of bilayers with untilted hydrocarbon chains packed in a hexagonal lattice in the plane of the bilayer (Tardieu et al., 1973). Since the lamellar repeat period for C(18):C(10)PC is unusually small (44 Å at 10% water content) and since the sharp symmetric wide-angle reflection is not usually observed for hydrated phosphatidylcholines, we investigated this lipid phase further. The sharp 4.11-Å wide-angle reflection was recorded for all gel specimens with 10% water content or more. However, at 5% water content, sharp wide-angle reflections were observed at 4.35, 3.87, 3.12, 2.44, 2.31, and 2.18 Å (data not shown). These reflections index on a rectangular lattice with dimensions a = 5.26 Å and b = 7.74 Å. The lamellar repeat periods for C(18):C(10)PC bilayers at 13 °C, as a function of water content, are shown in Figure 2. The repeat period, d, at 5% water is 54.5 Å. However, at 10% water d decreases over 10 Å to 44.2 Å. From 10% to 40% water, d increases monotonically to about 59 Å, where it levels off as an excess water phase forms for greater than 40% water.

Table I: X-ray Diffraction Parameters for C(18):C(10)PC[a]

% water	temp (°C)	d (Å)	d_l (Å)	d_f (Å)	S (Å^2)	d_s (Å)	$\sum$ (Å^2)	$S/\sum$
40	13	59.3	35.4	23.9	59.5	4.11	19.5	3.05
	22	68.4	41.0	27.4	54.9	4.6		
35	13	56.6	35.9	20.7	58.6	4.11	19.5	3.01
	22	63.5	41.3	22.2	54.6	4.6		
30	13	55.1	37.8	17.3	55.7	4.11	19.5	2.86
	22	57.9	40.5	17.4	55.6	4.6		
25	13	51.8	38.2	13.6	55.2	4.11	19.5	2.82
	22	54.6	40.9	13.7	55.0	4.6		
20	13	50.4	39.8	10.6	52.9	4.11	19.5	2.72
	22	51.0	40.8	10.2	55.2	4.6		
10	13	44.0	39.3	4.7	53.6	4.11	19.5	2.75
	22	48.8	43.9	4.9	51.3	4.6		
5	13	54.5	51.6	2.9	40.8	3.87	20.4	2.00
						4.35		

[a] d is the lamellar repeat period, d_l is the partial lipid thickness calculated from eq 1, d_f is the fluid layer thickness calculated from eq 2, S is area per lipid head group at the interface as calculated from eq 3, d_s is the short- or wide-angle spacing, and $\sum$ is the area per hydrocarbon chain determined from d_s (see text).

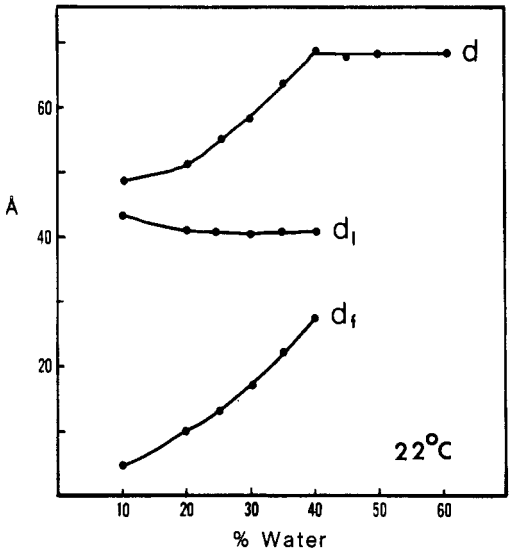

FIGURE 3: Repeat period (d), partial thickness of lipid bilayer (d_l), and fluid layer thickness (d_f) for C(18):C(10)PC at 22 °C.

For liquid-crystalline C(18):C(10)PC multilayers at 22 °C, the repeat period increases monotonically from 49 Å at 10% water to 68 Å at 40% water and then levels off as further water is added (Figure 3). For C(18):C(10)PC at 22 °C the wide-angle diffraction pattern consists of a single broad reflection at 4.6 Å, characteristic of liquid-crystalline lipid (Tardieu et al., 1973).

Since the concentration C (weight of lipid per weight of lipid plus water) of the sample is known, it is possible to determine the partial thickness of the lipid layer, d_l, the width of the fluid layer, d_f, and the average area available to one lipid molecule at the lipid–water interface, S, by the following formulas (Luzzati, 1968):

$$d_l = d\left(1 + \frac{\bar{v}_f}{\bar{v}_l}\frac{1-c}{c}\right)^{-1} \quad (1)$$

$$d_f = d - d_l \quad (2)$$

$$S = \frac{2M_r\bar{v}_l}{d(N \times 10^{-24})} \quad (3)$$

where $\bar{v}_f$ and $\bar{v}_l$ are the partial specific volumes of water and lipid, respectively, M_r is the molecular weight of the lipid, and N is Avagadro's number. For $\bar{v}_l$ we used 0.935 mL/g in the gel state and 1.0 mL/g in the liquid-crystalline state. The gel-state value is the same as that used by Tardieu et al. (1973) for C(18):C(10)PC at low water content, and both gel and liquid-crystalline values of $\bar{v}_l$ are consistent with specific volumes for symmetric saturated phosphatidylcholines measured by Nagle & Wilkinson (1978). The values for d_l and d_f for gel and liquid-crystalline state C(18):C(10)PC are shown in Figures 2 and 3, respectively. A noteworthy feature of these calculations is that the lipid layer thickness, d_l, is greater for the liquid-crystalline state than for the gel state. The fluid layer thickness are the same for gel and liquid-crystalline state, except near the excess water region where d_f is slightly greater for the liquid-crystalline phase.

The values for area per molecule at the interface, S, are shown in Table I. For the gel state, at 10% water content and above, where the hydrocarbon chains are in a hexagonal lattice, the area per hydrocarbon chain, $\sum$, can be calculated from the wide angle spacing, d_s = 4.11 Å, by the formula (Tardieu et al., 1973) $\sum = 2d_s^2/3^{1/2}$. As can be seen in Table I, the area per molecule, S, divided by the area per chain, $\sum$, is approximately equal to 3 for the gel-state phase at water contents of 10% and above. For the gel state at 5% water content, the dimensions of the rectangular unit cell give an area per hydrocarbon chain of $\sum = a(b/2) = 20.4$ Å^2. The area per molecule, S, calculated from eq 3 is 40.8 Å^2. Therefore, at 5% water content $S/\sum = 2.0$. For the fully hydrated liquid-crystalline state, S is about 55 Å^2, a somewhat smaller value than the 62 Å^2 determined for both C(14):C(14)PC at 37 °C (Janiak et al., 1979) and egg lecithin at 5 °C (Reiss-Husson, 1967) and significantly smaller than the 68 Å^2 calculated for egg lecithin at 25 °C (Reiss-Husson, 1967).

In order to calculate electron density profiles for gel-state C(18):C(10)PC, the phase angles for each reflection were determined by the swelling method (Moody, 1963; Worthington et al., 1973). Since this structure is centrosymmetric, each phase angle must be either 0 or π. Figure 4 shows structure amplitudes for the diffraction experiments at 13 °C between 10% and 50% water content. The swelling curve simplifies the determination of the phase angles, since for $0 < R < 0.10$ Å^{-1}, there are only three possible points (marked with arrows on Figure 4) where the transform could go through a zero and a phase-angle change could occur. That is, there are three regions in the structure amplitude curve denoted by numbers 1, 2, and 3 in Figure 4. There are $2^3 = 8$ possible phase angle combinations, since each of these regions can have a 0 or π phase. The sampling theorem (Shannon, 1949) was used to determine the correct phase combination. First, the structure factor at $R = 0$ was calculated for each phase-angle combination by the method of King & Worthington (1971).

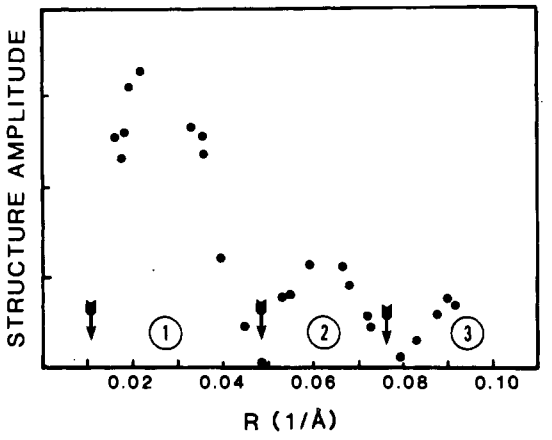

FIGURE 4: Structure amplitudes plotted vs. reciprocal space coordinate, R, for C(18):C(10)PC with 10–50% water at 13 °C. Arrows show possible zeroes and delimit regions 1, 2, and 3 in the transform.

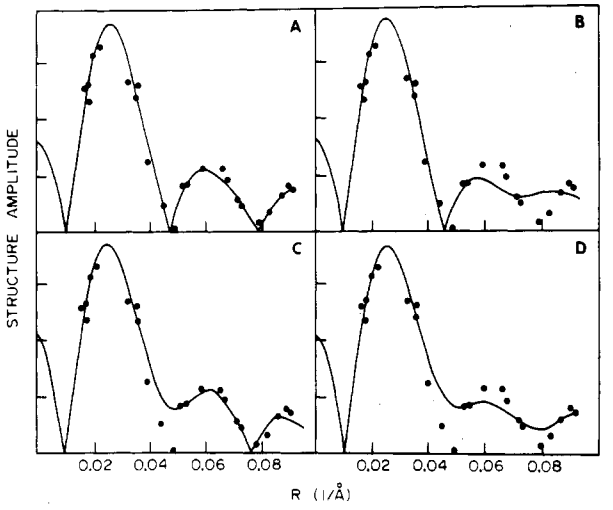

FIGURE 5: Absolute values of continuous transforms calculated by using the sampling theorem and (A) alternating phase angles for regions 1, 2, and 3, (B) regions 2 and 3 with the opposite phase angle of region 1, (C) regions 1 and 2 with the opposite phase of region 3, and (D) regions 1, 2, and 3 all with the same phase. Solid circles represent structure amplitudes as shown in Figure 4.

Next, the continuous transform was calculated for each possible phase-angle combination for each data set. The curves in Figure 5 are absolute values of one set of continuous transforms calculated for the particular data set at 30% water content. There are four curves shown, corresponding to alternative phase angles for the three regions (Figure 5A), the regions 2 and 3 having different phase angles than region 1 (Figure 5B), regions 1 and 2 having the opposite phase angle of region 3 (Figure 5C), and all regions having the same phase angle (Figure 5D). The curve in Figure 5A most closely fits the structure data (circles) for all regions of the transform. Thus, the correct phase-angle combination is (π, 0, π) or (0, π, 0) for regions 1, 2, and 3 of the transform. These two remaining possibilities can be distinguished by using the fact that the lipid hydrocarbon chains have a lower electron density than water. In order for the electron density profiles to reflect this, the phase choice must be (0, π, 0).

Figure 6 shows electron density profiles calculated by using these phase angles for C(18):C(10)PC at 10, 20, 30, and 40% water content. For all of these profiles, the low electron density region centered at 0 Å corresponds to the center of the hydrocarbon core of the bilayer. The high density peaks at about ±17 Å correspond to the lipid head groups, and the medium density regions on the outside of each profile correspond to

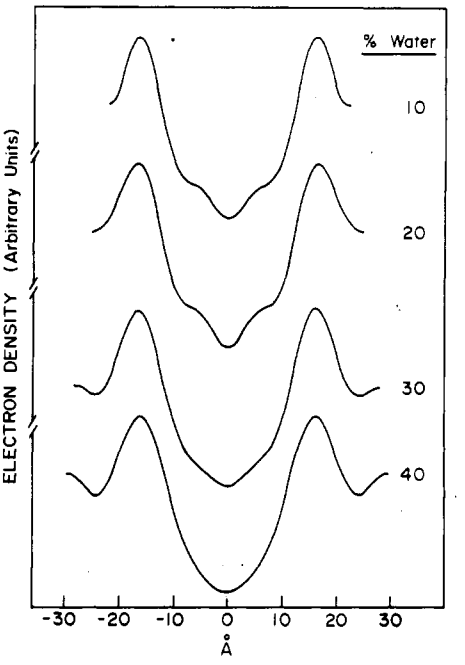

FIGURE 6: Electron density profiles for C(18):C(10)PC at 13 °C with 10, 20, 30, and 40% water in the multilayers.

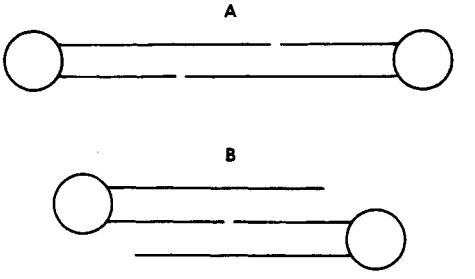

FIGURE 7: Two possible hydrocarbon chain configurations for C-(18):C(10)PC. Circles represent lipid head groups and straight lines represent hydrocarbon chains. In model A, which is consistent with the X-ray data for C(18):C(10)PC at 5% water content, the long and short chains from apposing molecules are aligned. There are two hydrocarbon chains per head group at the interface. In model B, which is consistent with the X-ray data for C(18):C(10)PC at 10% water content and above, the long chains span the width of the hydrocarbon region of the bilayer, and the short chains from apposing molecules are aligned. In model B there are three hydrocarbon chains per head group at the interfacial region.

the fluid layers between bilayer. As would be expected, fluid layers become wider with increasing percentage of water in the multilayers. The separation between head group peaks, d_{p-p}, in each of these profiles is between 33 and 34 Å. This can be compared to the partial thickness of the lipid layer, d_l, which is between 36 and 39 Å for these water contents (Figure 2). The observation that d_l is slightly larger than d_{p-p} is consistent with the data of Janiak et al. (1979), who found d_l varied between 47 and 42 Å and d_{p-p} was 40 Å for DMPC multilayers.

Discussion

The X-ray diffraction data indicate that hydrated C-(18):C(14)PC, when cooled below the pretransition temperature, forms the usual tilted gel-state phase, Lβ', comparable to gel states of symmetric saturated phosphotidylcholines such as C(14):C(14)PC, C(16):C(16)PC, and C(18):C(18)PC. However, the diffraction parameters are quite different for C(18):C(10)PC. The sharp wide-angle reflections indicate untilted hydrocarbon chains (Tardieu et al., 1973). For 5% water content, the values of $S/\sum = 2$ and $d_l = 51.6$ Å are

consistent with a "normal" bilayer (shown schematically in Figure 7A), as found at 1% water content by Tardieu et al. (1973) and suggested by Mason et al. (1981) on the basis of their calorimetry data. Molecular model building for this packing arrangement is consistent with this value of d_l. Moreover, this value of d_l = 51.6 Å is in excellent agreement with the lipid thickness Janiak et al. (1979) determined for hydrated C(14):C(14)PC, which has the same number of methylene groups as C(18):C(10)PC. Janiak et al. (1979) found d_l = 42.4 Å for maximally hydrated C(14):C(14)PC with a 35° chain tilt. Thus, C(14):C(14)PC with untilted chains would have a thickness of 51.8 Å.

As the water content of the multilayer system is increased from 5% to 10%, the hydrocarbon chain lattice in the plane of the bilayer changes from rectangular to hexagonal, d_l decreases by between 12 and 16 Å, and the ratio of $S/\sum$ changes to a value closer to 3 than to 2 (Table I). This value of $S/\sum \simeq 3$ is inconsistent with the usual bilayer hydrocarbon chain packing. For C(18):C(10)PC at 10% water content and above, we propose the packing arrangement shown in Figure 7B. In this model the C(18) chain extends across the width of the hydrocarbon region of the bilayer, and the C(10) chain aligns with the C(10) chain from the apposing lipid molecule. This packing arrangement has three hydrocarbon chains per lipid head group and thus accounts for the observed $S/\sum$ value of about 3. This model also is consistent with the observed values of d_l and d_{p-p}. To show this, we calculate the thickness of this bilayer of Figure 7B in a manner similar to that of Mason et al. (1981). An important point here is that in like-chain phosphatidylcholine bilayers the two acyl chains are conformationally inequivalent (Pearson & Pascher, 1979), since the initial segment of the *sn*-2 acyl chain is perpendicular to the *sn*-1 chain. This conformational inequivalence means that the *sn*-2 chain does not extend as far into the center of the bilayer as the *sn*-1 chain. By neutron diffraction, this difference has been estimated to be about 1.8 Å or 1.5 C–C bond lengths (Buldt et al., 1978; Zaccai et al., 1979), so that C(10) chain has an effective thickness of 8.5 C–C bonds. This implies that the effective thickness of the two apposing C(10) chains in our model would be the equivalent of about 17 C–C bonds plus the extra distance between apposing terminal methyl groups which is about 2 Å. This thickness matches very closely with the length of one fully extended C(18) *sn*-1 chain. Thus, the difference in thickness between bilayers of Figure 7A,B should be the difference between 26.5 C–C bonds [C(18) plus C(10) for Figure 7A] and 17 C–C bonds [C(10) plus C(10) for Figure 7B], which is 9.5 C–C bonds or about 12 Å. This compares favorably to the observed difference in d_l for 5% water and 10% water and above (Table I).

The value of d_{p-p} measured from the electron density profiles is about 34 Å. Using the value of 40 Å for tilted DMPC bilayers and considering the 35° tilt in C(14):C(14)PC bilayers (Janiak et al., 1979), we calculate a value for d_{p-p} = 48.8 Å for untilted C(14):C(14)PC bilayers. Thus, the d_{p-p} value for C(18):C(10)PC at 10% water and above is about 15 Å narrower than a normal, untilted lipid bilayer containing the same number of CH_2 groups. This again favors the model in Figure 7B which is 12 Å narrower than the model of Figure 7A. The shape of the electron density profiles, with a shallow terminal methyl dip in the center of the hydrocarbon region, is also consistent with the acyl chain arrangement of Figure 7B.

An important consideration in the organization of gel-state phosphatidylcholine bilayers is the relative cross-sectional area of the head group and lipid chains (McIntosh, 1980). Since the hydrated phosphatidylcholine head group lies approximately parallel to the bilayer plane (Franks, 1976; Buldt et al., 1978; McIntosh, 1978), it has a larger excluded area in the plane of the bilayer than the two gel-state chains and therefore would prevent straight chains from coming in close contact in the usual bilayer arrangement. In order for the chains to come closer together and thereby maximize van der Waals interactions, either the chains can tilt (McIntosh, 1980) as in C(16):C(16)PC (Tardieu et al., 1973) or C(18):C(14)PC (Figure 1) or the chains can partially interdigitate as in C(18):C(10)PC (Figure 7B). The following considerations show that the model of Figure 7B is energetically favorable compared to the usual tilted bilayer phase, providing there is a close match between the length of the long hydrocarbon chain which spans the bilayer core and the combined length of the two short chains which appose each other in the center of the bilayer. There is an energy cost, ΔE, in going from the standard bilayer configuration ($S/\sum$ = 2) to the bilayer of Figure 7B ($S/\sum$ = 3) because the terminal methyl end of the long hydrocarbon chain is exposed to interfacial water in Figure 7B. To approximate this energy, we use the formula $\Delta E = \gamma \Delta A N$ (Nagle, 1980), where γ is the interfacial surface pressure, ΔA is the additional area of hydrocarbon exposed to water, and N is Avagodro's number. For γ, we use a value of 30 dyn/cm (Evans & Waugh, 1977), and for ΔA we use 32.3 Å^2, which is the surface area of half a sphere whose volume is equal to a terminal methyl group. This value of ΔA was calculated by assuming that the volume of a methyl group is approximately twice the volume of a methylene group (Tardieu et al., 1973). The volume of a methylene group is 1.25 Å times the cross-sectional area of a chain, $\sum$. Thus, we calculate that the energy cost in exposing one terminal methyl to water is about 1.4 kcal/mol. However, there is a gain in van der Waals energy on going to the packing arrangement of Figure 7B, as the value of d_s and the area per chain, $\sum$, are less for this phase than for a normal bilayer phase. To quantitate this difference, we use eq 5 of Nagle & Wilkinson (1978) and compare the internal energy for a normal, hydrated tilted phosphatidylcholine bilayer, which has a double wide-angle reflection at 4.21 and 4.10 Å (each hydrocarbon chain has four neighbors at a distance of 4.86 Å and two neighbors at a distance of 4.74 Å) and the hydrated C(18):C(10)PC bilayer which has a single wide-angle reflection at 4.11 Å (each hydrocarbon chain has six nearest neighbors at a distance of 4.75 Å). The van der Waals energy gained by going to the closer packed phase shown in Figure 7B is about 2.8 kcal/mol. The Raman spectroscopy data of Huang et al. (1983) indicate that the below the phase transition temperatures C(18):C(10)PC has approximately the same number of gauche bonds as C(18):C(18)PC and fewer gauche bonds than C(18):C(14)PC. Therefore, the energy due to rotameric degrees of freedom of gel-state C(18):C(10)PC is less than or approximately equal to that of tilted phosphatidylcholines. Thus, since other energy contributions are small for hydrated phosphatidylcholines (Nagle, 1980) and since the van der Waals energy gained is larger than the energy cost exposing the methyl end of the C(18) chain to water, it is energetically favorable for hydrated C(18):C(10)PC to pack in the conformation shown in Figure 7B. However, since the energy cost in moving the long hydrocarbon chain to the interface is directly related to the area of hydrocarbon exposed to the water, the match between the length of the long chain and the sum of two short chains is critical. If the long chain were too long, or too short, additional hydrocarbon would come in contact with water and the usual tilted bilayer ($L\beta'$) phase would form. Thus, hydrated C-

(18):C(14)PC forms a tilted bilayer phase.

At 5% water content C(18):C(10)PC forms an untilted bilayer phase (Figure 7A). A possible explanation for this is that as the water content of the bilayer decreases, lipid head groups, in each monolayer as well as from adjacent bilayers, move closer together. Thus, the attractive dipolar forces between head groups, which are relatively small for fully hydrated bilayers (Nagle, 1980), become much larger. These forces act to increase the density of head groups, and at 5% water content, these head group interactions must shift the energy balance so that the phase shown in Figure 7A becomes energetically favorable.

The calorimetry data of Mason et al. (1981) and the Raman spectroscopy data of Huang et al. (1983) for C(18):C(10)PC are explained by the gel-state model of Figure 7B. The close packing of the acyl chains in this model would produce an unusually large transition entropy as well as relatively low values for gel-state intramolecular and interchain disorder.

The model of Figure 7B is also consistent with the unusual melting properties of C(18):C(10)PC bilayers (Table I). In normal bilayers, the lipid thickness decreases as the area per molecule increases upon melting. However, for the gel-state packing arrangement of Figure 7B where $S/\sum = 3$ as well as for fully interdigitated gel state bilayers where $S/\sum = 4$ (Ranck et al., 1977; McDaniel et al., 1983; McIntosh et al., 1983), the area per molecule decreases, and the lipid thickness increases upon melting. This is because, although the area per hydrocarbon chain increases in going to the more disordered liquid-crystalline state, the number of chains per head group decreases to the normal bilayer value of 2 (see below). Thus, upon melting, noninterdigitated gel-state bilayers decrease in thickness about 10 Å (Janiak et al., 1979), fully interdigitated gel-state bilayers increase about 10 Å in thickness (Ranck et al., 1977; McDaniel et al., 1983), and the partially interdigitated gel phase of C(18):C(10)PC (Figure 7B) increases 3–5 Å in thickness.

In the liquid-crystalline state, the fluidity of the lipid hydrocarbon chains makes it difficult to construct precise molecular packing models. However, our X-ray data coupled with the Raman data of Huang et al. (1983) allow for a fairly detailed picture of the hydrocarbon chain organization. Several lines of evidence indicate that the gel packing arrangement of Figure 7B converts to a normal liquid-crystalline Lα bilayer with two fluid chains per head group. First, as described above, d_1 increases while S decreases upon melting. Second, the values of d_1 and S are similar for liquid-crystalline C(18):C(10)PC and C(14):C(14)PC. At limiting water content $d_1 = 41$ Å and $S = 55$ Å^2 for C(18):C(10)PC (Table I) and $d_1 = 36$ Å and $S = 62$ Å^2 for C(14):C(14)PC (Janiak et al., 1979). Moreover, the increase in d_1 upon melting shows that the melted C(10) chains can no longer be in register or else there would be energetically unfavorable void volumes in the center of the bilayer. Similarly, if the C(18) chains were aligned there would be large voids near the bilayer center at the ends of the C(10) chains. There are two possible ways the lipid molecules could pack in the liquid-crystalline state to fill the potential void volumes and maximize van der Waals interactions. First, the C(18) chain could cross the center of the bilayer and fill the void at the end of a C(10) chain in the apposing monolayer. Second, the C(18) chain could bend and fill a void at the end of a neighboring C(10) chain in the same monolayer. In the liquid-crystalline state the acyl chains are relatively fluid, and both of these events probably occur. However, since the area per molecule for C(18):C(10)PC is slightly smaller than other liquid-crystalline phosphatidylcholine bilayers and since the Raman data (Huang et al., 1983) indicate that the intramolecular and interchain disorder are similar for melted C(18):C(10)PC and C(18):C(18)PC bilayers, there cannot be an unusually large number of gauche conformers in melted C(18):C(10)PC as the second possibility would suggest. Therefore, it appears likely that there is a significant amount of interpenetration of chains from apposing monolayers in the liquid-crystalline phase of C(18):C(10)PC. The data of Lewis & Engelman (1983) indicate that the thickness of the hydrocarbon region of liquid-crystalline phosphatidylcholine bilayers increases about 1 Å for each additional CH_2 group in the bilayer. Thus, for C(18):C(10)PC bilayers in the liquid-crystalline phase where there is a mismatch in chains of eight CH_2 groups, there could be as much as 8 Å of chain overlap from apposing molecules. This interdigitation would tend to couple the two monolayers of the bilayer, meaning that the physical properties of the bilayer would be different than those of a monolayer. That is, in the case of mixed-chain lipids, monolayers at air–water interfaces may not be equivalent to each monolayer of the bilayer.

In summary, the packing model shown in Figure 7B is unique in that there are three acyl chains per lipid head group at the interfacial region. In this phase, the hydrocarbon chains are packed more closely together than in normal hydrated phosphatidylcholine bilayers, explaining why there is an unusually large entropy change upon melting for C(18):C(10)PC bilayers (Mason et al., 1981).

After this paper was submitted for publication, Dr. Ching-hsien Huang, University of Virginia, sent us a copy of a paper (Hui et al., 1984) which analyzes the structure of mixed-chain lecithins by freeze–fracture and X-ray diffraction techniques. In that paper they have arrived at a similar packing model to ours for gel-state C(18):C(10)PC but a different packing model than ours for gel-state C(18):C(14)PC.

Acknowledgments

We thank Dr. William Longley for helpful discussions and Pat Thompson for an excellent job of typing the manuscript.

Registry No. C(18):C(10)PC, 78119-50-3; C(18):C(14)PC, 20664-02-2.

References

Barenholz, Y., & Thompson, T. E. (1980) *Biochim. Biophys. Acta 604*, 129–158.

Buldt, G., Gally, H. U., Seelig, A., Seelig, J., & Zaccai, G. (1978) *Nature (London) 271*, 182–184.

Calhoun, W. I., & Shipley, G. G. (1979) *Biochim. Biophys. Acta 555*, 436–441.

DeVries, G. H., & Norton, W. T. (1974) *J. Neurochem. 22*, 251–257.

Evans, E. A., & Waugh, R. (1977) *J. Colloid Interface Sci. 60*, 286–298.

Franks, N. P. (1976) *J. Mol. 100*, 345–358.

Huang, C., Mason, J. T., & Levin, I. W. (1983) *Biochemistry 22*, 2775–2780.

Hui, S. W., Mason, J. T., & Huang, C. (1984) *Biochemistry* (in press).

Janiak, M. J., Small, D. M., & Shipley, G. G. (1979) *J. Biol. Chem. 254*, 6068–6078.

King, G. I., & Worthington, C. R. (1971) *Phys. Lett. A 35A*, 259.

Lewis, B. A., & Engelman, D. M. (1983) *J. Mol. Biol. 166*, 211–217.

Luzzati, V. (1968) in *Biological Membranes* (Chapman D., Ed.), p 71, Academic Press, London and New York.

Mason, J. T., Huang, C., & Biltonen, R. L. (1981) *Biochemistry 20*, 6086–6097.
McIntosh, T. J. (1978) *Biochim. Biophys. Acta 649*, 325–335.
McIntosh, T. J. (1980) *Biophys. J. 29*, 237–246.
McIntosh, T. J., McDaniel, R. V., & Simon, S. A. (1983) *Biochim. Biophys. Acta 731*, 109–114.
McIntosh, T. J., Simon, S. A., Ellington, J. C., & Porter, N. A. (1984) *Biophys. J. 45*, 41a.
Moody, M. F. (1963) *Science (Washington, D.C.) 142*, 1173–1174.
Nagle, J. F. (1980) *Annu. Rev. Phys. Chem. 31*, 157–195.
Nagle, J. F., & Wilkinson, D. A. (1978) *Biophys. J. 23*, 159–176.
O'Brien, J. S., & Rouser, G. (1964) *J. Lipid Res. 5*, 339–342.
Pearson, R. H., & Pascher, I. (1979) *Nature (London) 281*, 499–501.
Ranck, J. L., Keira, T., & Luzzati, V. (1977) *Biochim. Biophys. Acta 488*, 432–441.
Reiss-Husson, F. (1967) *J. Mol. Biol. 25*, 363–382.
Shannon, C. E. (1949) *Proc. Inst. Radio Eng. N.Y. 37*, 10–21.
Tardieu, A., Luzzati, V., & Reman, F. C. (1973) *J. Mol. Biol. 75*, 711–733.
Worthington, C. R., King, G. I., & McIntosh, T. J. (1973) *Biophys. J. 13*, 480–494.
Zaccai, G., Buldt, G., Seelig, A., & Seelig, J. (1979) *J. Mol. Biol. 134*, 693–706.

Lateral Diffusion of Plastocyanin in Multilamellar Mixed-Lipid Bilayers Studied by Fluorescence Recovery after Photobleaching†

M. Fragata,* S. Ohnishi, K. Asada, T. Ito, and M. Takahashi

ABSTRACT: The lateral diffusion of fluoresceinyl isothiocyanate labeled plastocyanin (FITC-PCY) from spinach chloroplasts reconstituted into egg yolk phosphatidylcholine (PCh) bilayer membranes with and without stearylamine (SA) was examined by using fluorescence recovery after photobleaching. SA was included in the membranes to simulate a positively charged surface for the binding of plastocyanin, which behaves as an anion at pH 7.4 used throughout this work. As a reference, the lateral diffusion of the probe *N*-(7-nitro-2,1,3-benzoxadiazol-4-yl)phosphatidylethanolamine (NBD-PE) was also studied in the same bilayer systems. The diffusion coefficient (D) of NBD-PE in PCh bilayers was found to be (4.4 ± 0.4) × 10^{-8} cm^2/s at 296 K in agreement with results published in the literature for experiments run at comparable temperatures (287–298 K). In mixed PCh–SA (5:1) bilayers, however, D is (6.4 ± 0.5) × 10^{-8} cm^2/s. On the one hand, it is noted that the diffusion of FITC-PCY in PCh and PCh–SA bilayers cannot fit the theory for a single diffusion coefficient. Plotting the data according to the expression for a multicomponent system reveals the presence of at least one fast-moving and one slow-moving species. In PCh bilayers, D_{fast} ~ (4.9 ± 0.8) × 10^{-8} cm^2/s and D_{slow} ~ (8.1 ± 0.2) × 10^{-10} cm^2/s. In PCh–SA bilayers, D_{fast} ~ (6.3 ± 0.7) × 10^{-8} cm^2 and D_{slow} ~ (7.9 ± 0.3) × 10^{-10} cm^2/s. This shows that the D_{fast} values do not differ appreciably from the diffusivities determined for NBD-PE. Another interesting point is that the slow-moving species seems to be insensitive to the presence of SA in the bilayer. On the other hand, treatment of the plastocyanin samples with dithiothreitol (DTT), a reducing agent that hinders the formation of plastocyanin dimers, has the effect of changing the relative contents of the fast and slow species, i.e., $[PCY_{fast}]/[PCY_{slow}]$, from about 3.1 (nontreated samples) to 11.5 (DTT-treated samples). This is a good indication that the fast-moving species is a monomer whereas the slow-moving species is an aggregated form. Finally, comparing the D_{slow} values with a two-dimensional diffusion coefficient of ca. 2 × 10^{-9} cm^2/s estimated by Takano [Takano, M., Takahashi, M. A., & Asada, K. (1982) *Arch. Biochem. Biophys. 218*, 369–375] for the diffusion of plastocyanin in the thylakoid membrane, we suggest that the electron donor to $P700^+$ in vivo is most probably an aggregated form of the molecule.

In green plants and algae, the electron-transport sequence between photosystem II (PS II)[1] and photosystem I (PS I) starts with a photoinduced electron transfer from a chlorophyll special pair (Katz et al., 1978; Shipman et al., 1976) to a primary acceptor and ends with the reduction of $P700^+$, the reaction-center chlorophyll of PS I (Sauer, 1975). The electron donor to $P700^+$ is plastocyanin, a "blue" copper protein that has been found to function either at the internal surface of the thylakoid membrane (Haehnel et al., 1981) between cytochrome *f* and the P700 complex (Avron & Shneyour, 1971; Haehnel et al., 1980) or in the stroma membrane (K. Asada, M. A. Takahashi, and M. Takano, personnal communication). Monomeric PCY has a single type 1 Cu atom buried in a pocket surrounded by six to seven hydrophobic residues (Colman et al., 1978; Freeman, 1981). Another important feature of the molecule is a negatively charged patch; in poplar plastocyanin, for instance, it spreads from residues 42–44 to residues 59–61 (Colman et al., 1978). Of particular interest is the suggestion that the anionic hydrophilic patch and the

† From the Department of Biophysics (S.O. and T.I.) and the Research Institute for Food Science (K.A. and M.T.), Kyoto University, Kyoto, Japan, and the Centre de recherche en photobiophysique, Université du Québec à Trois-Rivières, Trois-Rivières, Québec, Canada G9A 5H7 (M.F.). *Received June 17, 1983; revised manuscript received March 16, 1984.*

[1] Abbreviations: DMPC, dimyristoylphosphatidylcholine; DTT, dithiothreitol; FITC, fluoresceinyl isothiocyanate; FITC-PCY, FITC-labeled plastocyanin; FRAP, fluorescence recovery after photobleaching; NBD-PE, *N*-(7-nitro-2,1,3-benzoxadiazol-4-yl)phosphatidylethanolamine; PCh, egg yolk phosphatidylcholine; PCY, plastocyanin; PS I, photosystem I; PS II, photosystem II; SA, stearylamine; cyt, cytochrome; Tris-HCl, tris(hydroxymethyl)aminomethane hydrochloride.

0006-2960/84/0423-4044$01.50/0